

Wave Compensator Design Based on Adaptive FFT Prediction Algorithm and H^∞ filtering

MingXi Zhang, Qi Li*, XiangDong Meng, YuQing He, HaiTao Luo

State Key Laboratory of Robotics
Shenyang Institute of Automation, Chinese Academy of Sciences
Shenyang 110200, P R China
lq12131010@163.com

Abstract - As the performance of the unmanned aerial vehicle (UAV) has been greatly improved with the rapid development of science and technology, the UAVs have been widely used for a broad range of applications. In recent years, the shipborne UAV has received considerable attention due to its low cost, small size, and high cost-effectiveness ratio. A key difficulty for the shipborne UAV is that due to the effect of the waves, the vertical sway, horizontal sway, and heave motions of the ships brought great challenges to the safe take-off and landing of the shipborne UAVs. To circumvent this drawback, this study proposed a wave compensation system based on the adaptive fast Fourier transform (FFT) prediction algorithm and H^∞ filtering. On the one hand, in order to reduce the time delay errors caused by sensors, controllers, and other devices, the FFT was adopted to construct an adaptive wave prediction algorithm. With the help of this algorithm, the heave motion model of the waves is forecasted to compensate the waves as synchronously as possible. On the other hand, in order to improve the robustness of the system and reduce external disturbances, the H^∞ filter was used to eliminate the high-frequency wave interference and make the compensation platform move more smoothly. Using the control and computation simulation software Matlab and the visual scene simulation software Vortex, based on the adaptive FFT prediction algorithm and H^∞ filtering, the co-simulation platform was constructed for the take-off and landing structural platform, the three-degree-of-freedom wave simulation, and the six-degrees-of-freedom wave compensation. The examples presented demonstrated that the proposed wave compensation system has feasibility in the take-off and landing of the shipborne UAVs. The examples also verified that the adaptive FFT prediction algorithm could forecast the waves effectively, and H^∞ filter has a good filtering effect in the wave compensation.

Index Terms - Adaptive FFT; wave prediction; H^∞ filtering; wave compensation

I. INTRODUCTION

The unmanned aerial vehicle (UAV) is a complex integrated system that requires the support of the aircraft design, the space positioning, the path planning, the flight control, and landing assistance. In recent years, the control technology for the autonomous mobile platforms on the sea, such as unmanned ships, becomes more and more mature. In the modern war, as UAVs play an irreplaceable role in the sea, and the technology of the autonomous take-off and landing becomes more important in the filed of UAVs. Because of the

randomness and time-varying nature of waves, the vertical and horizontal swing and heave motions of the ships brought great challenges to the safe take-off and landing of shipborne UAVs. It is of great significance to develop wave compensation platforms which can insulate against the interference of sea waves [1-3].

At present, the wave compensation platforms may be classified into the passive heave compensation platform (PHC) and the active heave compensation platform (AHC), and the hybrid active-passive system [4]. Regardless of the type of the wave compensation platforms, the goal of compensation platforms is to separate the load motion from the ship's motion. The simplest compensation is using a parallel set of spring-damper systems, located in the center between the lifting device and the load. As shown in Fig.1, a small vessel makes use of a passive heave compensation system to carry cargo. The system has the advantages of a simple structure and no energy input.

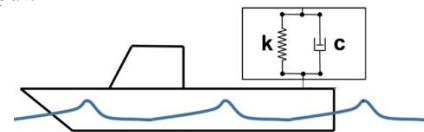


Fig. 1 PHC system example

Compared with open-loop passive compensation systems, active heave compensation systems involve closed-loop control and require energy input. The active system measures the lift motion of the ship, then passes it to the controller which moves the corresponding device to compensate the heave motion. Its greatest advantage is that the feedback variable is not limited to the heave motion of the ship. Robichaux and Hatleskog [5] adopted the microprocessors as a control system in 1993, which have a high adaptability and can be used in different ships. However, the type of control systems has a certain time delay. In 2012, Kyllingstad [6] used PID control to correct the time delay of the entire system by using a transfer function filter to improve the time delay. Kuchler et al. [7] applied a heave prediction algorithm to predict the heave motion of ship based on previously measured motion data, and then used these predicted motions to perform the platform control. The course of the design and test of the wave compensation systems is with high unknown

uncertainty and very expensive cost, while the simulation system has the advantages of high repeatability, economy, safety, etc. Therefore, the simulation technology has been greatly developed in recent years. In 2009, Jong-Chun et al. [8] developed a three-degree-of-freedom wave simulation system that can simulate waves in different sea areas using a variety of wave spectrum. In 2010, Piyang Jun [9] built a ship motion simulator by means of a 6-DOF parallel platform and a joint FFT algorithm.

Despite the success of the above wave compensation systems, the controller and the hardware device of the existing wave compensation systems, including active compensation systems and passive compensation systems, have poor adaptability, and can not automatically adjust the control parameters for sea waves in different natural environments. And the vibration of systems caused by the motion of the hardware and the high frequency disturbances of sea waves, makes the system with less robustness. To circumvent this drawback, this study proposed a wave compensation system based on the adaptive fast Fourier transform (FFT) prediction algorithm and H_∞ filtering. In this study, for achieving the purpose of synchronous compensating the waves, the wave disturbances obtained by the FFT are decomposed in real time, then the adaptive Kalman filter is used to construct the wave prediction algorithm to reduce the errors caused by the time delay of sensors, controllers, etc. On the other hand, for the vibration caused by high-frequency noise, The H_∞ filter was used to eliminate the high-frequency interference of the waves and smooths the motion of the compensation platform. Considering the complexity of the marine environment and the high degree of unknown uncertainty, in this work Vortex, Qt, OSG, and other simulation tools was used to construct a co-simulation system based on a parallel six-degrees-of-freedom wave compensation platform and a three-degrees-of-freedom wave simulation platform.

II. PROBLEM STATEMENT

The simulation method for complex systems has many advantages such as high repeatability, low expense, and safety. Due to the complexity of testing environment of the sea surface and the high expense of the experimental study, this work uses a variety of simulation tools such as Vortex, Qt, and OSG to build a co-simulation system constructed by the parallel six-degrees-of-freedom wave compensation simulation platform and a serial three-degrees-of-freedom wave simulation platform. The serial three-degrees-of-freedom wave simulation platform was used to simulate the waves, while the parallel six-degrees-of-freedom wave compensation simulation platform was used to simulate the real wave compensation platform. We could use the co-simulation system to perform simulation tests for control strategies and the wave prediction method. Especially, we proposed a wave compensation control strategy based on the adaptive FFT prediction algorithm and the H_∞ filtering.

The co-simulation system consists of three subsystems: wave compensation platform, ocean wave simulation

platform, and human-computer interaction interface, as shown in Fig. 2.

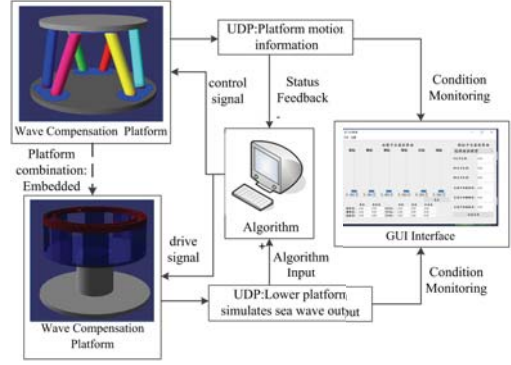


Fig. 2 The co-simulation system

Table 1 List of system main parameters

the parallel six-degrees-of-freedom wave compensation platform	Supporting load weight	$\geq 1000\text{Kg}$	Platform size	$5\text{m} \times 5\text{m} \times 2.2\text{m}$
	Angle range	Yaw angle: $\leq \pm 25^\circ$ Pitch angle: $\leq \pm 20^\circ$ Rolling angle: $\leq \pm 20^\circ$	Accuracy of angular displacement	Yaw angle : 0.1° Pitch angle : 0.1° Rolling angle : 0.1°
	Angular speed range	Yaw angle : $\geq \pm 20^\circ/\text{s}$ Pitch angle : $\geq \pm 15^\circ/\text{s}$ Rolling angle : $\geq \pm 15^\circ/\text{s}$	Displacement range	Yaw : $\leq \pm 0.5\text{m}$ Pitch : $\leq \pm 0.6\text{m}$ Rolling : $\leq \pm 0.6\text{m}$
	Displacement speed	lifting : $\geq \pm 0.2\text{m}/\text{s}$ Longitudinal : $\geq \pm 0.2\text{m}/\text{s}$ Rolling : $\geq \pm 0.2\text{m}/\text{s}$		
Three-degrees-of-freedom wave platform	Simulated Wave Height	$\leq 2.5\text{m}$	Pitch Angle Range	$\leq \pm 20^\circ$
	Rolling angle range	$\leq \pm 20^\circ$	Vertical moving range	$\leq \pm 1.5$
	Rotary speed	$\leq \pm 20^\circ/\text{s}$	moving speed	$\leq \pm 0.5\text{m}/\text{s}$

Taking the advantage of Vortex simulation software, the active wave compensation platform with Stewart structure and the RRP series wave simulation platform for three degrees-of-freedom can be constructed. The main parameters of these two platforms can be seen in Table 1. The simulation platform can simulate waves up to 2.5m in height. The compensation platform could be calculated and controlled by the simulation computer in real time using Matlab software. The GUI interface provides a good human-computer interaction scene, which can more directly reflect the operating status of the system.

Compared with the passive wave compensation platform, the active wave compensation platform has a more precise structure and its control algorithm is more complex. However, the active wave compensation platform has a significant time delay, which will seriously affect the compensation performance for the waves, and even cause the system to lose stability. For this reason, it is very necessary to design a wave compensation algorithm with predictive performance that can identify and correct the time delay of the waves in time. Moreover, the waves have a strong time-varying and random nature, and the high-frequency component of the waves may strongly disturb the performance of the hardware and software equipment of the system, resulting in infinite drift of the displacement and severely reducing the robustness of the system.

In order to remedy the above mentioned drawbacks, in this work, firstly we designs the self-adaptive FFT prediction to estimate the sea wave interference, then we used the H_∞ filter to filter the interference signal, and finally we applied the self-adaptive FFT prediction and the H_∞ filter to the sea wave compensation co-simulation system to verify these techniques and simulate the wave compensation platform system.

III. THE STRATEGY OF CONTROL

The wave active compensation controller mainly makes use of the combination of H_∞ filtering and FFT prediction. The filter could filter out the high frequency interference of waves for a general controlled object composed of internal models of the subsystems. The FFT algorithm is used to predict the disturbances of sea waves before T time. The expansion and contraction of platform cylinder was controlled by taking advantage of the 6-DOF solution of the obtained by Matlab software, to achieve the goal of active compensation of sea waves. The structure of controller was shown in Fig 3.

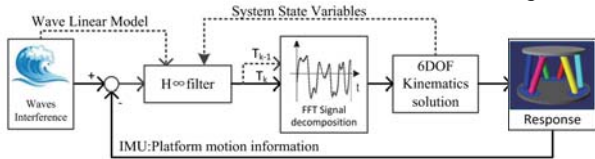


Fig. 3 The structure of controller for active compensator

III.1 Kinematic Analysis of 6-DOF Platform

In order to describe the upper platform motion clearly, two coordinate systems O and W are defined as shown in Fig. 4. Suppose that $q_m = [x \ y \ z]^T$, $q_r = [\alpha \ \beta \ \gamma]^T$. In the

base coordinate system O, the coordinate value of A_i may be obtained by

$$A_i = \begin{bmatrix} X_A \\ Y_A \\ Z_A \end{bmatrix}_i = \begin{bmatrix} rc\theta_i^A c\alpha c\beta + rs\theta_i^A (c\alpha s\beta s\gamma - s\alpha c\gamma) \\ rc\theta_i^A s\alpha c\beta + rs\theta_i^A (s\alpha s\beta s\gamma + c\alpha c\gamma) \\ -rs\theta_i^A s\beta + rs\theta_i^A c\beta s\gamma \end{bmatrix} + q_m, \quad (1)$$

where $r = |A_i w|$ denotes the effective radius of the upper platform, θ_i^A denotes the angle between $A_i w$ and X_w , w denotes the center point of the upper platform. c represents \cos function, and s represents \sin function.

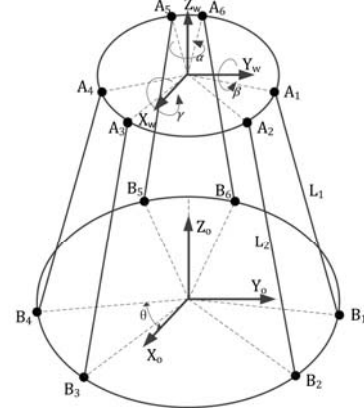


Fig. 4 diagram of 6-DOF platform

The coordinate value of B_i in the O coordinate system could be given by:

$$B_i = [X_B \ Y_B \ Z_B]_i^T = [Rc\theta_i^B \ Rs\theta_i^B \ 0]^T, \quad (2)$$

where $R = |B_i o|$ denotes the effective radius of the lower platform, θ_i^B denotes the angle between $\theta_i^B o$ and X_o , and o represents the center point of the lower platform. The inverse Jacobian matrix for the situations of the upper platform and the six cylinders can be expressed as:

$$J^{-1} = \left(\frac{\partial L_i}{\partial q_j} \right)_{6 \times 6}, i, j = 1, 2, \dots, 6, \quad (3)$$

where $\frac{\partial L_i}{\partial q_j} = \frac{\partial |A_i B_i|}{\partial q_j}$, and $A_i B_i$ represents the distance between point A_i and B_i . To this point, from above equations, the forward kinematics solution can be obtained by the numerical iteration method.

III.2 Signal preprocessing based on H_∞ Filter

The system diagram was converted into a standard LFT diagram form as shown in Fig. 5, in which the general controlled object was determined.

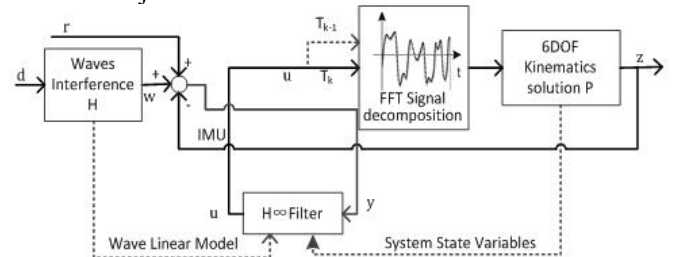


Fig. 5 The diagram of H_∞ filtering problem

The state space [10] may be expressed as:

$$\begin{aligned} \dot{x} &= Ax + B_1w + B_2u \\ z &= C_1x + D_{11}w + D_{12}u \\ y &= C_2x + D_{21}w + D_{22}u \end{aligned} \quad (4)$$

The transfer function matrix of the general controlled object G could be given by

$$G = \begin{bmatrix} 0 & 0 & KP \\ 1 & H & -KP \end{bmatrix} \quad (5)$$

in which, the waves was described by a linear model, and P can be obtained by (1)-(2). K represents the fast Fourier transform. The transfer function can be expressed as:

$$H = h(s) = \frac{2\xi\omega_0\sigma_w s}{s^2 + 2\xi\omega_0 s + \omega_0^2}, \quad (6)$$

where σ_w denotes the sea wave intensity constant, ξ is the damping coefficient, ω_0 is the dominant wave frequency. And in the state space, the the transfer function matrix could be given by :

$$G = \begin{bmatrix} A & B_1 & B_2 \\ C_1 & D_{11} & D_{12} \\ C_2 & D_{21} & D_{22} \end{bmatrix}. \quad (7)$$

By solving the following Riccati algebraic equations,

$$AX + XA^T - X[C_2^T C_2 - \gamma^{-2} C_1^T C_1]X + B_1 B_1^T = 0, \quad (8)$$

the minimum allowable value of γ and the corresponding symmetric matrix X are determined. In the above equation, the sufficient condition of existence of the solution to the equation is that the corresponding Hamiltonian matrix H does not have any eigenvalue on the imaginary axis. So, the coefficient matrix corresponding to the state space of the H_∞ filter may be determined by

$$A_f = A - X C_2^T C_2 B_f = X C_2^T, \quad C_f = C_1, \quad D_f = 0. \quad (9)$$

III.3 Adaptive FFT Algorithm Design

As the undulating motion of the ships caused by the waves is not disorganized, it depends on the dynamics of the hull and the state of the sea, which makes it possible to predict the waves for relatively long portions of time. The heave motion of waves can be expressed as the sum of a set of harmonic waves (also called modal) with different periods, as shown in the following equation [11]:

$$w(t) = \left(\sum_{i=1}^N A_i \sin(2\pi f_i t + \varphi_i) \right) + \rho(t), \quad (i = 1, \dots, N \quad t_0 \leq t \leq T), \quad (10)$$

A_i , f_i , φ_i , respectively, represents the amplitude, frequency, and phase of the i th harmonic. $\rho(t)$ indicates the initial compensation value of the wave signal. The overall structure of the algorithm was shown in Fig.6.

First, applied the fast Fourier transform to the filtered time signal $w(t)$ in ΔT to obtain the amplitude and phase frequency data of the input signal; then, the main N harmonic functions, their corresponding amplitudes A_{FFT} , frequencies f_{FFT} , and phase φ_{FFT} were identified by the peak detector. In order to improve the accuracy of identification and prediction for the waves, in this work a state estimator was constructed based on the Kalman filtering principle. By comparing the latest measured values with the estimated values, the parameters of harmonic waves were updated online in real

time. And the wave signals after T_{pre} time could be accurate prediction.

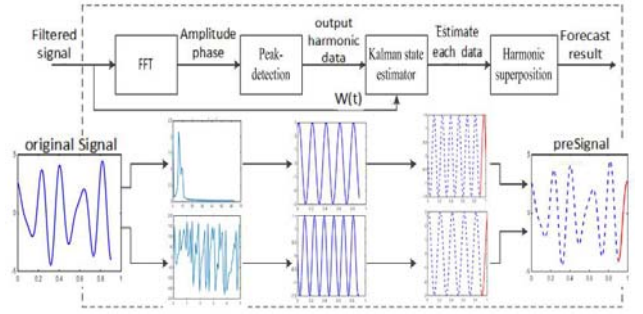


Fig. 6 diagram of prediction algorithm

Then the Eq. (4) can be converted into the form of ordinary differential equation as follows:

$$\dot{x} = A_i x = \begin{pmatrix} 0 & 1 \\ -(2\pi f_i)^2 & 0 \end{pmatrix} x, \quad (11)$$

$$x(t_0) = x_{0,i} = \begin{pmatrix} A_i \sin(\varphi_i) \\ 2\pi A_i f_i \cos(\varphi_i) \end{pmatrix}, \quad (12)$$

$$w_i = C_i x = (1 \ 0) x \quad i = 1, \dots, N, \quad (13)$$

in which $t_0 \leq t \leq t_0 + \Delta T$. Considering the sum of N harmonic waves and adding the initial compensation value, the system state equation could be given by:

$$\dot{x} = Ax = \begin{bmatrix} A_1 & 0 & \dots & \dots & 0 \\ 0 & A_2 & \ddots & & \vdots \\ \vdots & \ddots & \ddots & \ddots & \vdots \\ \vdots & & & A_N & 0 \\ 0 & \dots & \dots & 0 & 0 \end{bmatrix} x, \quad x(t_0) = x_0 = \begin{bmatrix} x_{0,1} \\ x_{0,2} \\ \vdots \\ x_{0,N} \\ \rho(t) \end{bmatrix}, \quad (14)$$

Using the Kalman filter, the amplitude $A_{i,t}$ and phase $\varphi_{i,t}$ for each frequency may be predicted by the following equation

$$\hat{\dot{x}} = A\hat{x} + L(w - \hat{w}), \quad (15)$$

$$\hat{w} = C\hat{x}, \quad (16)$$

where L represents the Kalman filter gain matrix, which can be determined by

$$L = PC^T R^{-1} \quad (17)$$

in which P is the solution to the Riccati equation:

$$PC^T R^{-1} CP - AP - PA^T - Q = 0, \quad (18)$$

where, Q denotes the input white noise covariance matrix, R denotes the measured white noise covariance matrix. Then harmonic parameters of different frequencies can be estimated by Kalman filtering as follows

$$\hat{x}_{1,i}(t) = A_{Obs,i} \sin(2\pi f_{FFT,i} t + \varphi_{Obs,i}), \quad (19)$$

$$\hat{x}_{2,i}(t) = 2\pi A_{Obs,i} f_{FFT,i} \cos(2\pi f_{FFT,i} t + \varphi_{Obs,i}). \quad (20)$$

Each parameter in the above equation can be calculated as follows:

$$f_{Obs,i} = f_{FFT,i}, \quad (21)$$

$$\varphi_{Obs,i} = \arctan\left(\frac{\hat{x}_{1,i}(T)}{\hat{x}_{2,i}(T)}\right) - 2\pi f_{FFT,i} T, \quad (22)$$

$$A_{Obs,i} = \frac{\hat{x}_{1,i}(T)}{\sin(2\pi f_{FFT,i} T + \varphi_{Obs,i})}. \quad (23)$$

Up to now, the prediction wave signals can be expressed as the sum of the harmonic waves with different frequency,

$$w_{pre}(t) = \left(\sum_{i=1}^N A_{Obs,i} \sin(2\pi f_{Obs,i} t + \varphi_{Obs,i}) \right) + \rho(t),$$

$$(i = 1, \dots, N \quad T \leq t \leq T_{pre}), \quad (24)$$

in which $\rho(t)$ can be calculated by

$$\rho(t) = \hat{x}_{2N+1}(T), \quad T \leq t \leq T_{pre} \quad (25)$$

IV. SIMULATION AND EXPERIMENT

Sea waves are irregular waves generated by sea wind. According to long-term studies on waves, it shows that sea waves can be analyzed using theoretical knowledge of stationary random processes. In this work, the ITTC double-parameter spectrum was used as the wave simulation density function as follows [12]:

$$S_{\xi}(\omega) = \frac{0.78}{\omega^5} \exp\left(-\frac{3.12}{\bar{\xi}_{w/3}^2 \omega^4}\right) \quad (26)$$

in which $\bar{\xi}_{w/3}$ denotes the average wave height of harmonic waves, and ω denotes the corresponding frequency of each harmonic waves. For example, in the case of the fourth sea wind, the single-point long-wave wave is simulated as shown in Fig.7.

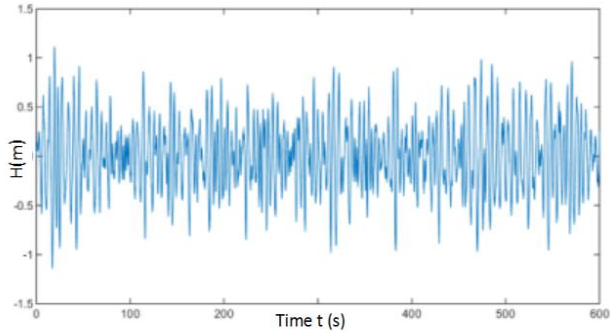


Fig. 7 ITTC wave spectrum simulation of the fourth level wind

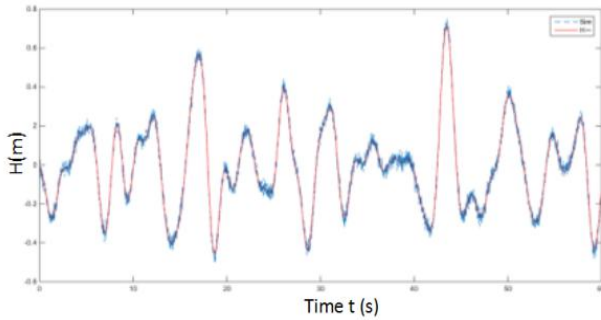


Fig. 8 the effect of the H_{∞} filter

With H_{∞} filter method, the sea wave input was preprocessed by the high-frequency filter. It can be seen from Fig.8 that the filter has obvious filtering effect, and can filter more than 90% of the high-frequency signal above 0.5 Hz, and the filter can effectively reduce the interference for the device, improve the robustness of the system.

Combining the a three-degree-of-freedom wave simulator with the real-time simulation algorithm for ship deck movements, the wave compensation simulation system shown in Fig. 9 was constructed, in which the subsystem on the bottom of the system is the wave simulation platform,

while the subsystem on the top of the system is the wave compensation simulation subsystem.

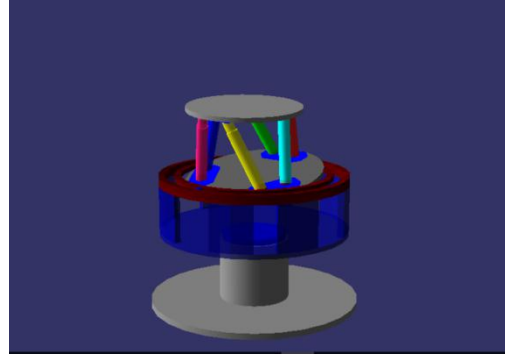


Fig. 9 the wave compensation simulation system

Firstly, the platform step test was performed for the compensator: the wave simulation platform was controlled to generate a step signal in the vertical Z direction, and at the same time, the output of the H_{∞} filter and track of the top platform motion were measured, as shown in Fig. 10. It can be seen that the H_{∞} filter is very effect for tracking, and the top platform can compensate in time and has a strong real-time performance.

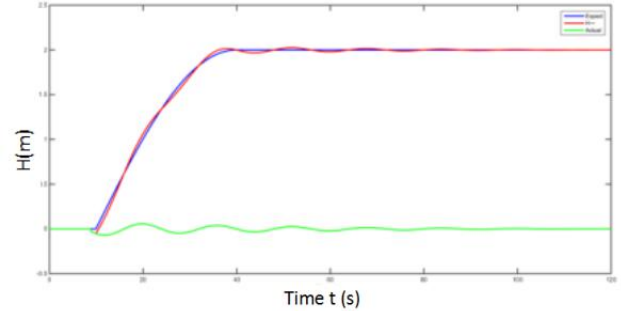


Fig. 10 The compensator step test

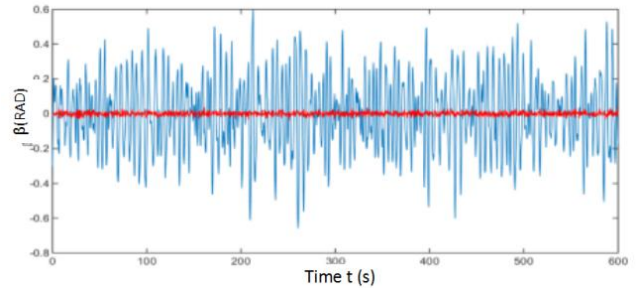


Fig. 11 the comparison of the curves of movement of the pitch γ of the upper and lower bases

When the wave simulation system used the ITTC wave spectrum to simulate the sea wave motion, the upper six-degree-of-freedom compensation system performed the wave compensation and extracted the pitch, roll, and vertical Z motion curves of the upper and lower circular bases of the compensation subsystem, as shown in Figs. 11-13.

As can be seen from the above three figures, the wave compensation controller designed in this study has a very good wave compensation function and can decouple the motion of

three degrees-of-freedom of the waves in pitch, roll and vertical in time and accurately. Making use of the wave compensator, the interference of ships caused by the sea waves could be significantly improved.

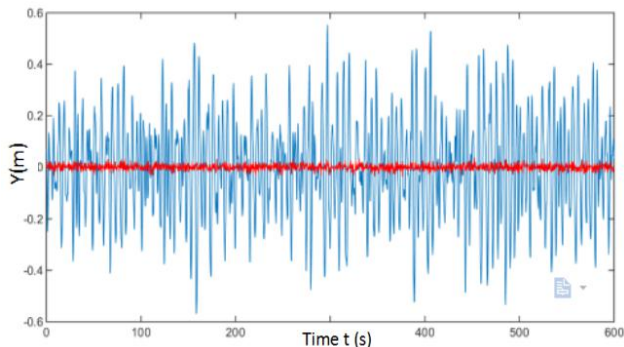


Fig. 12 comparison of the curves of movement of the roll angle β of the upper and lower bases

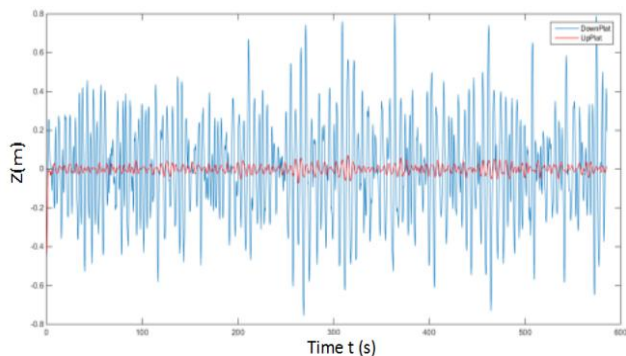


Fig. 13 the comparison of the curves of vertical Z movement of the upper and lower Bases

V. CONCLUSION

In this work, based on the adaptive FFT prediction algorithm, and H_∞ filtering, the co-simulation platform was constructed for the take-off and landing structural platform, which can be used for the real-time compensation of sea waves below the fourth level wind. The system has two subsystems, the three-degree-of-freedom wave simulation subsystem and the six-degrees-of-freedom wave compensation subsystem. The examples presented demonstrated that the

subsystem and the six-degrees-of-freedom wave compensation subsystem. The examples presented demonstrated that the proposed wave compensator system has feasibility in the take-off and landing of the shipborne UAVs. The examples also verified that the adaptive FFT prediction algorithm could forecast the waves effectively, and H_∞ filter has a good filtering effect in the wave compensation.

ACKNOWLEDGMENT

This work was supported by the National Nature Science Foundation of the PR China (No. 11602283, U1608253, 91748130, 51505470) and the State Key Laboratory of Robotics (2017-Z17).

REFERENCES

- [1] Taoyu Jin, Peifeng Li, "Development and key technology of UAV" Aeronautical Manufacturing Technology, vol. 464, no.20, pp. 34-39, 2014.(in Chinese)
- [2] Xinqiang Jia, Peng Lin, MinWen Wang, "Study on disturbance of board movement in process carrier aircraft's landing and its compensation,"AERONAUTICAL COMPUTING TECHNIQUE, vol. 40, no.1, pp. 114-118, 2010.(in Chinese)
- [3] GuoZhong Dong,ShengShu Wang, ChunSheng hu "Unmanned Aerial Vehicle applications and trends,"NATIONAL DEFENSE SCIENCE & TECHNOLOGY, no.10, pp. 34-38, 2006.(in Chinese)
- [4] Woodacre J K, Bauer R J, Irani R A, "A review of vertical motion heave compensation systems," Ocean Engineering, vol. 104, pp. 140-154, 2015.
- [5] Robichaux, L.R., Hatleskog, J.T, "Semi-active heave compensation system for marine vessels," US Patent,1993..
- [6] Kyllingstad, A., "Method and apparatus for active heave compensation, September," US Patent, 2012.
- [7] Kuchler, S., Mahl, T., Neupert, J., Schneider, K., Sawodny, O., "Active control for an offshore crane using prediction of the vessels motion," . IEEE/ASME Trans. Mechatron," vol.16, no. 2, pp. 297-309, 2011. F
- [8] Jong-Chun P, Miyata H, Ooga T, et al."Motion Simulation of a Sailing Boat in Oblique Waves with Three Degrees of Freedom,"Journal of the Japan Society of Naval Architects & Ocean Engineers, vol.2001, no. 190, pp. 191-199, 2009.
- [9] Pi, Yangjun, and X. Wang. "Observer-based cascade control of a 6-DOF parallel hydraulic manipulator in joint space coordinate, " Mechatronics, vol.20, no. 6, pp. 648-655, 2010. F
- [10]XinPing Wang H filter in thee disturbance of waves," thesis of Dalian Maritime University, 2003.(in Chinese)
- [11]Neupert J, Mahl T, Haessig B, et al. "A heave compensation approach for offshore cranes," American Control Conference. IEEE, pp.538-543, 2008.
- [12]JinBo Xu, XinqQian Bian, MingYu Fu,"Simulation of Sea Wave of Long-crested Wave and Spectral Estimation," Journal of Harbin University of Science and Technology, vol.4, pp.30-33, 2010.(in Chinese)